AD-A089 208 CALIFORNIA UNIV BERKELEY DEPT OF MATERIALS SCIENCE --ETC F/G 11/6
CLUSTER VARIATION STUDY OF ORDERING IN FCC SOLID SOLUTIONS.(U)
JUL 80 J M SANCHEZ, D D FONTAINE DAAG29-77-G-0002
UNCLASSIFIED UCB-ENG-DDF8001 ARO-14071.7-MS NL

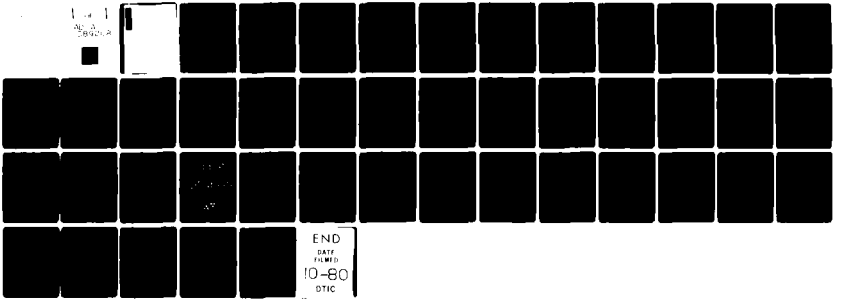

END
DATE FILMED
10-80
DTIC

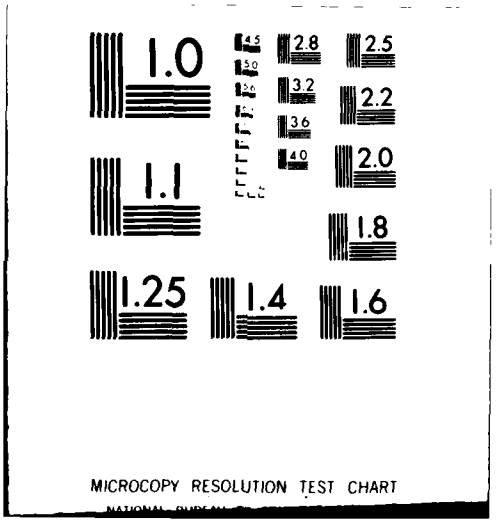
1.0
1.1
1.25
1.4
1.6
1.8
2.0
2.2
2.5
2.8
3.2
3.6
4.0
4.5
5.0
MICROCOPY RESOLUTION TEST CHART

(12) ARO (11) 14241.7-MS

SECURITY CLASSIFICATION OF THIS PAGE (When Data Entered)

REPORT DOCUMENTATION PAGE

READ INSTRUCTIONS BEFORE COMPLETING FORM

1. REPORT NUMBER (14) UCB-ENG-DDF8001	2. GOVT ACCESSION NO. AD-A089208
3. RECIPIENT'S CATALOG NUMBER	
4. TITLE (and Subtitle) (6) CLUSTER VARIATION STUDY OF ORDERING IN FCC SOLID SOLUTIONS	5. TYPE OF REPORT & PERIOD COVERED Final; 10/11/76-2/29/80
	6. PERFORMING ORG. REPORT NUMBER
7. AUTHOR(s) (10) J. M. Sanchez and D. de Fontaine	8. CONTRACT OR GRANT NUMBER(s) (15) DAAG29-77-G-0002 DAAG29-78-G-0058
9. PERFORMING ORGANIZATION NAME AND ADDRESS Department of Materials Science & Mineral Engineering, University of California, Berkeley, California 94720	10. PROGRAM ELEMENT, PROJECT, TASK AREA & WORK UNIT NUMBERS (12) 751
11. CONTROLLING OFFICE NAME AND ADDRESS U. S. Army Research Office Post Office Box 12211 Research Triangle Park, NC 27709	12. REPORT DATE (11) July 1980
	13. NUMBER OF PAGES 43
14. MONITORING AGENCY NAME & ADDRESS(if different from Controlling Office) (9) Final Rept. 11 Oct 76-31 Feb 80	15. SECURITY CLASS. (of this report) Unclassified
	15a. DECLASSIFICATION/DOWNGRADING SCHEDULE

16. DISTRIBUTION STATEMENT (of this Report)

Approved for public release; distribution unlimited.

17. DISTRIBUTION STATEMENT (of the abstract entered in Block 20, if different from Report)

18. SUPPLEMENTARY NOTES

THE VIEW, OPINIONS, AND/OR FINDINGS CONTAINED IN THIS REPORT ARE THOSE OF THE AUTHOR(S) AND SHOULD NOT BE CONSTRUED AS AN OFFICIAL DEPARTMENT OF THE ARMY POSITION, POLICY, OR DECISION, UNLESS SO DESIGNATED BY OTHER DOCUMENTATION.

19. KEY WORDS (Continue on reverse side if necessary and identify by block number)

Order-Disorder
Coherent equilibrium
Phase-Diagrams

20. ABSTRACT (Continue on reverse side if necessary and identify by block number)

A systematic approach to the calculation of coherent phase diagrams using high-level approximations of the Cluster Variation Method has been developed. The emphasis in this investigation was placed in higher than first neighbor interactions in order to treat the complex ordering observed in the Ni-V and Ni-Mo systems. The new Cluster Variation approximations, when applied to the Ising ferromagnet, yielded significant improvement on the results of previous applications of the theory. A new approach to the Ground State problem including pair and many-body interactions was also developed.

DD FORM 1 JAN 73 1473 EDITION OF 1 NOV 65 IS OBSOLETE 411829 Unclassified

SECURITY CLASSIFICATION OF THIS PAGE (When Data Entered)

1. FOREWORD (ABSTRACT)

A systematic approach to the calculation of coherent phase diagrams using high-level approximations of the Cluster Variation Method has been developed. The emphasis in this investigation was placed in higher than first neighbor interactions in order to treat the complex ordering observed in the Ni-V and Ni-Mo systems. The new Cluster Variation approximations, when applied to the Ising ferromagnet, yielded significant improvement on the results of previous applications of the theory. A new approach to the Ground State problem including pair and many-body interactions was also developed.

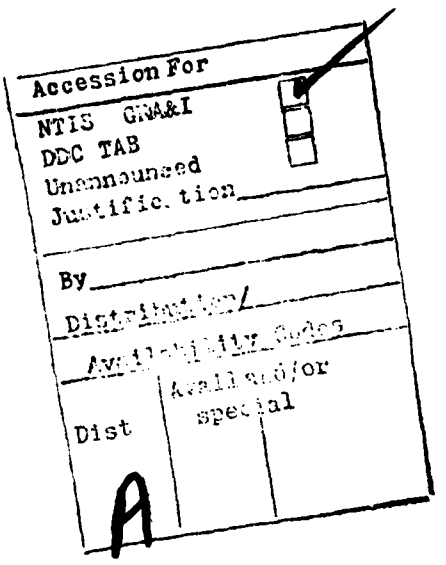

2. TABLE OF CONTENTS

3. LIST OF ILLUSTRATIONS AND TABLES

Figure 3: Ground-state diagram for negative first neighbor pair interaction (v_1). v_2 and v_6 refer, respectively, to second neighbor pair and octahedron many-body interactions.

Figure 4: The ordered superstructures of the <1½0> family.

Figure 5: Long-range order parameter for A_2B_2 phase at stochiometry ½.

Figure 6: Long-range order parameter for A_2B_2 phase off-stochiometry.

Figure 7: Long-range order parameter for A_3B phase at stochiometry ¼.

Figure 8: Long-range order parameter for A_3B phase off-stochiometry.

Figure 9: Temperature-concentration phase diagram for a ratio of first to second neighbor pair interaction of 0.25.

Figure 10: Relative stability of the A_2B phase for different values of the ratio of second to first neighbor pair interactions: a) ε=0.28, b) ε=0.3, and c) ε=0.33.

Figure 11: Variation of the temperature difference for the reactions disordered → A_2B_2 and A_2B_2 → A_2B with the ratio of first to second neighbor pair interactions ε.

Figure 12: Temperature-composition phase diagram for ε=0.35.

Figure 13: Temperature-composition phase diagram for ε=0.45.

4. BODY OF REPORT

4.1. Introduction

Equilibrium phase diagrams are widely recognized for their practical value in the design of alloys, the mechanical properties of which are greatly controlled by the microstructures of second phases. The microstructures in question, however, are seldom determined by equilibrium properties due to the fact that most metallurgical processes are carried out in far-from-equilibrium conditions resulting, for example, from the rapid quenching of a solid solution into metastable or even unstable regions of the phase diagram. Furthermore, the crystal lattice imposes a severe constraint on phase changes, particularly when such changes are associated with ordering and/or segregation: the coexistence of truly equilibrium phases will in most cases require the presence of cyrstalline defects, e.g. dislocation at incoherent interfaces which, however, can only be introduced late in the decomposition since their formation is mediated by diffusion and/or high internal stress fields. Thus, the first products of decomposition will be characterized by the fact that they share the same crystal lattice, allowing for small distortions, or are superstructures of the parent phase. Such initial products, usually referred to as coherent phases, develop fine and very homogeneous microstructures which, if not completely preserved, directly affect the microstructure of the final products.

The goal of this project has been to investigate the theoretical tools needed for the calculation of order-disorder coherent phase diagrams in fcc based binary solid solutions. Whereas equilibrium phase

diagrams can be determined experimentally or synthesized by fitting thermodynamic data with regular or subregular solution models, coherent phase diagrams are not in general amenable to either treatment. For the latter phase diagrams, it is possible to perform first principle statistical mechanics calculations which, at the present time, are not feasible for the determination of equilibrium or incoherent phase diagrams. Thus experiment and theory effectively complement each other, the former providing the incoherent and the latter the coherent phase diagrams, to produce a complete picture of the possible mechanism of decomposition in solid-solutions.

The method used for the free energy calculations throughout this work was the Cluster Variation Method (CVM) proposed by Dr. Kikuchi in 1951. An important aspect of our work is that the usefulness and feasibility of the CVM for the calculation of complex phase diagrams has been clearly established.

In order to develop free energy models, or approximations that are applicable to a significant number of ordered fcc superstructures, it has been recognized, since the work of Kanamori et al.[2] and of Cahn and co-workers[3], that at least second-neighbor pair interactions must be included in the ordering energy. Second neighbor pair interactions in fcc lattices had not been used in the past, however, and it was therefore necessary to develop the appropriate CVM approximations and to work with relatively large clusters and complicated superstructures. The need for large clusters posed a serious bookkeeping problem since, in the CVM, one must keep track of the probabilities of all cluster configurations. Thus, a simple scheme for working with a reduced set of

multisite correlation functions was developed (see Section 4.2 and Ref. 4). Such an approach suggested a concise and convenient manner of describing the state of order in binary solid solutions as points in the multidimensional configuration space of correlation functions. The configurational polyhedron introduced by Kudo and Katsura[5] can be easily defined in such multidimensional space of correlation functions, as explained in Section 4.5.7 and Ref. 6. Furthermore, the lowest energy superstructures, or Ground States, follow once the vertices of the configurational polyhedron are known.

Free energy expressions for different cluster approximations including first and second neighbor interactions were derived and tested in the case of the nearest neighbor Ising ferromagnet for which very reliable values of the critical temperature are known. These results are reported in Sections 4.3 and 4.4 and Ref. 4.

Among all the approximations tested, the tetrahedron-octahedron cluster combination was used in order to calculate order-disorder phase diagrams.

The starting point for phase diagram calculations by means of the CVM is the so-called Ground State problem (see Section 4.5.1 and Ref. 6), that is, one must determine all superstructures that will be realized in a given phase diagram and for a certain set of pair and/or many-body interactions. To proceed with the calculations one then chooses interaction energy parameters which, according to the ground-state analysis, will ensure the presence of the desired low temperature phases.

In the results discussed in Section 4.5.2 and Ref. 7, first and second neighbor interactions v_1 and v_2, respectively, with $v_1>0$ and

v_2/v_1 = 0.25 were used in order to guarantee the presence in the phase diagram of some of the characteristic ordered structures of the Ni-V system, namely the DO_{22} and the Ni_2V superstructures.

The final step in the calculation of the coherent phase diagram requires the minimization of the free energy functional for different values of the temperature and average concentration. The numerical calculations are somewhat involved providing, in addition to the coherent phase diagram, a very complete picture of the state of order. That is, long and short range order parameters, and in fact the probability distribution for all tetrahedron and octahedron cluster configurations, follow directly from the minimization procedure. By performing an instability analysis in reciprocal space one can calculate the mean square amplitude of the cluster probabilities which can be approximately related to experimentally determined short range order diffuse intensity. Furthermore the instability analysis yields the instability loci, or ordering spinodas, as it is discussed in detail in Section 4.5.2 and Ref. 7.

This preliminary investigation of ordering in fcc binary solid solutions was concluded with a study of the effect on the phase diagram of the ratio of second to first neighbor pair interactions in the range 0 to 0.5. The results are presented in Section 4.6.

Each of the items briefly sketched in the introduction will be expanded in more detail in the remaining sections of this report.

4.2. Cluster Algebra

When using the CVM, one is confronted with the cumbersome task of characterizing a generally large number of cluster probabilities. For example, in a binary alloy being described by an n-point cluster one

must keep record of 2^n probabilities. Due to the point group symmetry of the crystal lattice, however, there are definite constraints among the cluster probabilities; i.e., the number of independent configurational variables is considerably less than 2^n for an n-point cluster. One can therefore save much computational effort by establishing a set of independent configurational variables.

A given cluster of lattice points will be identified by a pair (n,s), where n refers to the number of points in the cluster and s is used to distinguish different n-point clusters; e.g., first and second neighbor pairs, different types of triangles, etc. Each point in the cluster can be occupied by any of the atomic species, let us say A and B for a binary solid solution. A particular distribution of A and B atoms on the n,s cluster will be referred to as a cluster configuration and it will be specified by a collective index J indicating the manner in which the cluster is populated, e.g., J = [1, -1, 1,...-1] where 1 and -1 stand for A and B, respectively.

Let $x_{n,s}(J)$ be the probability that the n,s cluster is in the J configuration, the total number of possible configurations being 2^n for a binary solid solution. As already mentioned, the probabilities associated with the 2^n configurations are not all independent due to the linear constraints which arise from the symmetry of the n,s cluster and of the crystalline phase. In order to obtain a set of independent configurational variables, we introduce the occupation operator

$$\Gamma_i(p) = \tfrac{1}{2}[1 + i\sigma_p] \qquad (1)$$

where σ_p takes values 1 or -1 if lattice point p is occupied by an A or a B atom, respectively, and where i equals 1 for A and -1 for B. Thus

$\Gamma_i(p)$ takes value 1 if p is occupied by an i-type atom and zero otherwise.

The probability $x_{n,s}(J)$ can then be calculated as:

$$x_{n,s}(J) = \Gamma_i(p)\,\Gamma_j(p')\ldots\Gamma_k(p'') \tag{2}$$

where p, p',...p" are n lattice vectors defining the n,s cluster, where J stands for the set [i, j...k] and where the brackets denote an ensemble average.

Using Equations (1) and (2) and expanding the products, one obtains

$$x_{n,s}(J) \equiv x_\ell(J) = \frac{1}{2^n}\left[1 + \sum_{\ell'} V_{\ell\ell'}(J)\,\xi_{\ell'}\right] \tag{3}$$

where, in order to simplify the notation, ℓ and ℓ' stand for the collective indices (n,s) and(n',s'), respectively, and where the multisite correlation function ξ_ℓ is given by:

$$\xi_\ell \equiv \xi_{n,s} = \langle\sigma_p\,\sigma_{p'}\ldots\sigma_{p''}\rangle. \tag{4}$$

The coefficients $V_{\ell\ell'}(J)$ in Equation (3) are given by sums of n'-order products of the i,j,...k (which take values ± 1) in the collective index J. The particular structure of the coefficients $V_{\ell\ell'}(J)$ can be best illustrated by an example: the probability for an i,j,k (where i,j,k is 1 for A and -1 for B) triplet of nearest neighbors is given by:

$$x_3(i,j,k) = \frac{1}{2^3}\left[1 + (i+j+k)\xi_1 + (ij+ik+jk)\xi_2 + (ijk)\xi_3\right] \tag{5}$$

where ξ_1, ξ_2, and ξ_3 are the point, nearest neighbor pair and triangle correlations, respectively. The coefficient $V_{31}(J) = i+j+k$ is obtained by summing, over all <u>points</u> in the triangle, the associated indices in configuration J. Likewise $V_{32}(J) = ij+jk+ik$ is obtained by summing over all <u>pairs</u> the associated product of indices. In general, the procedure is continued until all subclusters, including the cluster itself, are exhausted. For the 3-point cluster of Equation (5), the largest "subcluster" is the triangle itself and the coefficient $V_{33}(J)$ is just ijk.

In writing Equation (5), we have assumed the space group symmetry of the fcc lattice. For ordered superstructures, however, one must distinguish the value of the point correlation function on different lattice points, the value of pair correlations along different crystallographic directions, etc. The expression for the triplet probabilities, for example, will be slightly different from Equation (5). The procedure for determining all the independent multisite correlation functions and the coefficients $V_{\ell\ell'}(J)$, can be summarized as follows:

i) A multisite correlation function is associated with each distinct subcluster of the largest cluster (included), where two subclusters are said to be distinct if they are not related by a symmetry operation of the space group of the crystal under consideration. The multisite correlation functions thus defined give a set of independent configurational variables for the cluster approximation chosen.

ii) The coefficients $V_{\ell\ell'}(J)$ relating the probabilities $x_{n,s}(J)$ and the correlation functions $\xi_{n',s'}$ (see Equation 3) are obtained by summing over all n', s' cluster in n,s the associated n'-order products of the indices i,j...k in configuration J.

4.3. Higher Cluster Approximations

The central problem of the CVM is that of calculating approximate expressions for the number of configurations Ω of a crystal lattice having definite distribution of clusters (pairs, triads, etc.) of lattice points which may be, in general, occupied by any one of a given set of atomic "species".[1] The equilibrium cluster distribution is then determined by minimizing the free energy

$$F = E - TS = E - k_B T \ln\Omega$$

where E, a linear function of the cluster concentrations, is the energy

of the configuration in question and where S is the configurational entropy of the system.

Although it is found that larger clusters yield, in general, successively higher levels of approximations, the degree of difficulty involved in the minimization of the free energy increases sharply with the size of the basic cluster. Due to such difficulties, and despite the fact that the CVM represents a remarkable improvement over other approximate methods such as the molecular field and quasichemical approximations, only clusters containing a relatively small number of lattice points have been treated thus far. The CVM entropy associated with a number of higher cluster approximations have been derived in Ref. 4. Those which have been used for free energy calculations are:

a) The Tetrahedron-Octahedron (TO). This approximation consists in combining the nearest neighbor tetrahedron and the regular octahedron in fcc lattices. Since the clusters contain first and second neighbor pairs most fcc superstructures, in principle, can be described within this approximation.

b) The Double Tetrahedron-Octahedron (DTO). In this level of approximation the basic clusters are the regular octahedron as in a), and a cluster formed by two tetrahedrons joined by a nearest-neighbor pair. The DTO cluster combination is the largest cluster so far used for actual calculations in the CVM, and it allows up to third neighbor pair interactions in the configurational energy.

4.4. The Ising Ferromagnet

In order to test the reliability of the TO and DTO approximations, we calculated the critical temperature and specific heat for the fcc,

spin-½ Ising ferromagnet (see Ref. 4). The value of T_c obtained from different approximations and that calculated from a high temperature expansion are shown in Table I. Table II gives the coefficients of the expansion for the high temperature specific heat. The resulting value of T_c in the DTO approximation was only 1.5% higher than the one obtained from a high temperature expansion, and the expansion for the high temperature specific heat gave four coefficients exactly, the fifth one being determined to within 0.4%.

Thus the CVM yields useful approximate results, provided that large enough clusters are used, with far less computational labor than is commonly required with more precise theoretical methods. More importantly, the CVM, as handled here, allows the incorporation, in the energy expression, of second and third neighbor pair interactions and even many-body interactions with absolutely no additional difficulties. This is a very significant consideration since, as discussed in the Introduction, the stability of various ordered structures found experimentally in fcc and bcc binary alloys can only be demonstrated by appealing to higher than first-neighbor pair interactions. Hence clusters large enough to contain explicitly at least second neighbor distances must be used in the CVM calculations.

4.5. Order-Disorder Phase Diagrams

The program briefly outlined in the Introduction for the calculation of order-disorder phase diagrams, namely the determination of ground-states and the free energy minimization, was carried out in the TO approximation in fcc lattices.

4.5.1. The Ground State Problem

The cluster algebra presented in Section 4.2 provides a simple starting point for the study of ground states in binary solid solutions (See Ref. 6). In particular, requiring that the cluster probabilities defined by equation (3) be positive, a set of linear constraints given by:

$$1 + \sum_{\ell'} V_{\ell,\ell'}(J)\, \xi_{\ell'} > 0 \quad (J = 1 \ldots 2^n) \tag{6}$$

must be imposed on the multisite correlation functions.

The set of inequalities (6) together with the restriction $|\xi_\ell| < 1$, clearly imply that the configuration space is limited to a convex polyhedron: the so-called configurational polyhedron originally introduced by Kudō and Katsura.[5] The fact that the configurational polyhedron is convex allows us to write any state of order, represented by a vector $\underset{\sim}{\xi}$ whose components are the multisite correlation functions, in terms of the barycentric coordiantes ρ_k; namely:

$$\underset{\sim}{\xi} = \sum_{k=1}^{K} \rho_k\, \underset{\sim}{\xi}^{(k)} \tag{7}$$

where $\underset{\sim}{\xi}^{(k)}$ corresponds to one of the K vertices of the configurational polyhedron and where the ρ_k are non-negative numbers such that:

$$\sum_{k=1}^{K} \rho_k = 1 \tag{8}$$

The use of barycentric coordinates is very convenient for the minimization of the configurational energy and, therefore, for the determination of the ground-states. In a given approximation involving r distinct correlation functions, the most general form for the configurational energy is:

$$E = \sum_{\ell=1}^{r} v_\ell \, \xi_\ell \tag{9}$$

where the v_ℓ are effective ℓ-body interaction parameters.

Using Equations (7) and (9) we can write the configurational energy as:

$$E = \sum_{k=1}^{K} \rho_k \, E^{(k)} \tag{10}$$

where

$$E^{(k)} = \sum_{\ell=1}^{r} v_\ell \, \xi_\ell^{(k)} \tag{11}$$

is the configurational energy of the state represented by the vertex k.

In order to determine the ground states, one must minimize the energy E subject to the constraint of constant average concentration. In terms of the point correlation ξ_1, the average concentration constraint is:

$$\xi_1 = \sum_{k} \rho_k \, \xi_1^{(k)} \tag{12}$$

where $\xi_1^{(k)}$ is the point correlation of the k-th vertex. From Eqs. (8), (10) and the fact the $\rho_k > 0$, it follows that the unconstrained minima of the configurational energy will be located at the vertices of the configurational polyhedron. If the constraint of Eq. (12) is imposed, the state of minimum energy will correspond to a linear superposition of at most two vertices of the configurational polyhedron. The ground state problem is then reduced to: a) determining all vertices of the configurational polyhedron, and b) determining the range of the interaction parameters v_ℓ for which given vertices of the configurational polyhedron are ground states. The associated maps in interaction space, i.e., the space formed by the v_ℓ, will be called ground-state diagrams.

Both points a) and b) are difficult problems in linear programming for which a number of algorithms have recently been developed.[8] The vertex enumeration required in a), has been carried out for the TO approximation using a method based on the Simplex algorithm.

The results obtained can be summarized as follows. A total of 43 vertices were found, of which only 26 were truly distinct since there were 17 pair of vertices connected by the operation of exchanging the role of A and B atoms. Of the 26 distinct vertices, one corresponded to pure A (or B) atoms and 8 were associated with the ground-state superstructures known from previous investigations to be stable with first and second neighbor pair interactions only.[2,3] Thus, all the ground states originally predicted by Kanamori (see Table III) and confirmed by Cahn and coworkers in the first and second neighbor pair approximation for fcc lattices are, as one should expect, recovered in the present formulation.

There remained 17 vertices to be accounted for. One can show that, with the cluster probabilities associated with 10 of these vertices, it is not possible to construct fcc superstructures. The fact that certain vertices of the configurational polyhedron are not superstructures is a general limitation of the method, rooted in the fact that the linear constraints of Eq. (6) are in terms of average concentrations for small clusters which cannot ensure an either A- or B- only occupancy at the lattice points. Finally we were able to associate the remaining 7 vertices with fcc superstructures. The superstructures in question are listed in Table IV and their associated unit cells are shown in Fig. (1).

The final step in the characterization of the ground-states, consists in the determination of the so-called ground-state diagrams. Such

diagrams define regions in interaction space in which different sets of ordered superstructures will be ground states. Two examples of ground-state diagrams are shown in Figs. (2) and (3), where v_1 and v_2 stand, respectively, for first and second neighbor pair interactions and where v_6 is the octahedron interaction. The remaining energy parameters were taken equal to zero. The first neighbor pair interaction energy v_1 is, respectively, positive and negative for Fig. (2) and Fig. (3). Finally, the different regions on the diagrams have been labelled by a prototype superstructure, when possible, or by the ground-state superstructures designated according to Table III and Fig. (1).

4.5.2. Prototype Phase Diagram

In order to keep the number of parameters as low as possible, only first and second neighbor pair interactions will be considered. Working with a reduced temperature scale τ defined as the absolute temperature T normalized by v_1/k with v_1 the first neighbor interaction energy and k Boltzman's constant, there is only one physical parameter in our calculation, namely the ratio $\varepsilon = v_2/v_1$ with v_2 the second neighbor pair interaction energy. Three cases can be distinguished depending on the ratio ε. These three cases are conveniently classified in terms of families of ordered structures labeled by the point in reciprocal space where the Fourier transform of the pairwise energy has its absolute minimum. Such families are: (i) the <100> family for $\varepsilon < 0$, (ii) $\langle \frac{1}{2}\frac{1}{2}\frac{1}{2} \rangle$ family for $\varepsilon > \frac{1}{2}$, and (iii) the $\langle 1\frac{1}{2}0 \rangle$ family for $0 < \varepsilon < \frac{1}{2}$. The ground-state ordered superstructures belonging to each family are summarized in Table III where the space group and, when applicable, the structure information and examples are given.

As seen in Table III, the <1½0> family comprises six different ordered structures. At stochiometry 1/3, there are three different degenerate structures: A_2B, A_2B', and A_2B'' (see Table III). The A_2B' and A_2B'' structures together with that of the A_5B phase at stoichiometry 1/6, have monoclinic Bravais lattices.

Calculations were carried out for the following ground-state superstructures of the <1½0> family: (i) the A_2B_2 phase with space group $I4_1/amd$, (ii) the A_2B phase with space group Immm, and (iii) the A_3B phase with space group I4/mmm. The three structures above have a particularly simplifying feature in common: they can be formally obtained by stacking of (420) lattice planes which are either occupied entirely by A or by B atoms. On the other hand, the remaining <1½0> superstructures, namely, the monoclinics A_2B', A_2B'', and A_5B cannot be obtained by stacking of pure A or B (420) planes. Due to the fact that low symmetry makes actual computations a cumbersome undertaking and that the structures in question do not seem to be realized in nature, we did not consider them further in this work. The particular sequences of planes for the A_2B_2, A_2B, and A_3B superstructures are schematically shown in Fig. 4 together with a (001) projection of their respective unit cells.

Included in Fig. 4 is the Dla structure with stochiometry 1/5 (A_4B) and space group I4/m. The Dla structure, an example of which is Ni_4Mo, is not a ground state in the first and second neighbors energy model used here, but it is degenerate with a mixture of the A_3B (DO_{22}) and the monoclinic A_5B phases of the <1½0> family. Nonetheless, the A_4B phase was included in our study since it can also be obtained by stacking

pure A or B (420) planes. The A_4B phase was found to be unstable for the particular value of second to first neighbor interaction-energy ratio of 0.25 and temperature range used in our calculations. Such finding clearly emphasizes the importance of a detailed analysis of the ground-state problem prior to CVM calculations.

The derivation and form of the free energy in the TO approximation for the <1½0> family is highly technical and will not be reproduced here, the interested reader being referred to Ref. 7. Depending on the symmetry of the phase under consideration, the number of correlation functions needed to describe the state of order in the TO approximation varies. Since the free energy functional must be minimized with respect to the correlation functions in order to obtain the equilibrium state, the size of the numerical problem to be solved also varies from phase to phase. The number of non-linear algebraic equations to be solved for the disordered, A_2B_2, A_2B and A_3B phases were respectively 10, 33, 46 and 45. Representative plots of the long range order parameters for the different ordered phases are shown in Figs. 5-8. Note that for the A_3B phase two ordered parameters, namely the amplitude of compositional waves of wave vector <100> and <1½0>, are needed. Furthermore the discontinuity in the order parameter characteristic of first order transitions observed near stochiometry A_3B (Fig. 7) is not present in Fig. (8), indicating a second-order transition.

The calculated phase diagram is shown in Fig. 9. Characteristic features in the phase diagram are the tricritical points labeled T_1, T_2 and T_3—where second and first order transitions meet—and the bicritical point B at the junction of two second order and a first order

transitions. The so-called ordering spinodal, corresponding to the concentration-temperature loci at which the disordered solution becomes unstable, is also shown in Fig. 9 (broken line).

4.6. The effect of varying interatomic pair interactions

The calculated coherent phase diagram described in Section 5 can be regarded as a prototype for coherent ordering in Ni-V, Au-Cr and Ni-Mo, for example. As mentioned in the introduction, coherent phase diagrams are in general not available experimentally and therefore a detailed comparison with real systems is not possible at the present time. Nevertheless, it is of interest to study the effect of the ratio of second to first neighbor pair interaction energy (ε) on the relative stability of the different ordered phases.

For the value of $\varepsilon = 0.25$ used to calculate the phase diagram of Fig. 9, the A_2B ordered phase is seen to become stable over a very narrow phase field and at very low temperatures. In order to raise the ordering temperature of the A_2B phase with respect to that of the DO_{22} (A_3B) structure, the value of ε was systematically varied within the range 0 to 0.5. Figure 10 shows a portion of the temperature-chemical potential phase diagram in the neighborhood of the bicritical point B (see Fig. 9), for values of ε equal to 0.28, 0.3 and 0.33. Figure 11 shows a plot of the difference in ordering temperatures for the fcc disordered (α) $\rightarrow A_2B_2$ and the $A_2B_2 \rightarrow A_2B$ reactions near the A_2B stochiometry as a function of the ratio α. Figure 11 suggests that the reaction $\alpha \rightarrow A_2B$ takes place only for values of ε larger than 1/3. Since the $\alpha \rightarrow A_2B$ reaction takes place in the NiV system and apparently does not in NiMo, one can infer that the latter system is characterized by small values of ε whereas in the former the value of ε should be larger than 1/3.

Temperature-composition phase diagrams were calculated for $\varepsilon = 0.35$ and for $\varepsilon = 0.45$. The results are shown in Figs. 12 and 13. A complicated topology is observed for $\varepsilon = 0.35$, the phase diagram displaying a number of multicritical points. It is unknown to the authors whether the features of the phase diagram in Fig. 13 has been detected either in alloys or in antiferromagnetic systems.

A much simpler topology is achieved by increasing ε to 0.45 as it can be seen in Fig. 13. The dominant feature is now the increased stability of the A_2B over larger temperature and composition ranges. Thus the phase diagram of Fig. 13 can be considered as prototype for coherent ordering in Ni-V systems.

Simple inspection of the equilibrium Ni-V phase diagram suggest, however, that the coherent phase diagram may be considerably more complicated than that of Fig. 13. In fact it is not expected that the simple interaction energy model used here, namely constant first and second neighbor interaction energies, will accurately account for real systems. In fact, as shown by de Fontaine and Kikuchi,[9] even for the simpler case of Cu-Au one must rely on many-body interactions in order to obtain a reasonable fitting to the phase diagram.

4.7. Conclusion

The problem of ab-initio phase diagram calculations remains one of the great challenges of modern solid-state physics and statistical mechanics. The prospect of being able to predict a phase diagram is at the same time very attractive to the materials scientist since most macroscopic properties can ultimately be related to the equilibrium phase diagram.

It has been the main objective of this work to investigate the feasibility of such phase diagram calculations. To begin with, it was essential to formulate the problem in such a manner that, without becoming utterly unrealistic, it could be solvable. Thus we limited ourselves to the study of coherent phase diagrams and, furthermore, we assumed that the configurational energy was given in terms of constant-pairs and/or many-body interactions, the values of which, hopefully, will be provided in the future by the solid-state physicists. In this manner we could concentrate on the thermodynamic and statistical mechanics aspects of the problem. Out of a number of approximate techniques available to calculate coherent phase diagrams we choose the CVM for a variety of reasons. Among them is that althought the CVM is a classical "mean field" theory it provides remarkably accurate results, away from critical regions, with much less computational difficulties than more elaborate techniques such as Renormalization Group Theory. Of course the use of regular or subregular solution models was not considered in our work since such models are very poor approximations, valuable mainly for the rationalization of thermodynamical data. Thus the CVM is an intermediate alternative between the very sophisticated methods of modern statistical mechanics and the very empirical approach based in free energy fitting by regular or subregular solution models.

Some of the attractive technical features of the cluster method used in our investigation can be summarized as follows:

1) The method provides a simple description of the state of order in terms of a finite number of multisite correlation functions.
2) The Ground-State problem is concisely formulated as that of enumerating the vertices of the so-called configurational polyhedron.

3) A hierarchy of increasingly more accurate approximations can be generated by using larger cluster sizes in the CVM free energy.

4) Instability and fluctuation analysis can be carried out in reciprocal space.

Although the calculation of coherent phase diagrams for complex superstructures and large cluster approximations are in general tedious, they are also, as we have proved, feasible and fundamentally simple. The development of more systematic approaches to the problem of minimizing the free energy and the implementation of more efficient computer codes will undoubtedly broaden the field of application of CVM in the future. We feel that with this work the first important step in that direction has been taken.

5. BIBLIOGRAPHY

1. R. Kikuchi, Phys. Rev., 81, 998 (1951).

2. J. Kanamori, Prog. Theor. Phys., 35, 66 (1966); J. Kanamori and Y. Kakehashi, J. Phys. (Paris), 38, C7-274 (1977); M. Kaburagi and J. Kanamori, Prog. Theor. Phys., 54, 30 (1975).

3. M. J. Richards and J. W. Cahn, Acta Metall., 19, 1263 (1971); S. M. Allen and J. W. Cahn, Acta Metall., 20, 423 (1972).

4. J. M. Sanchez and D. de Fontaine, Phys. Rev. B, 17, 2926 (1978).

5. T. Kudō and S. Katsura, Prog. Theor. Phys., 56, 435 (1976).

6. J. M. Sanchez and D. de Fontaine, to appear in Structure and Bonding in Crystals, M. O'Keeffe and A. Navrotsky, Eds., Academic Press, New York (1980).

7. J. M. Sanchez and D. de Fontaine, Phys. Rev. B, 21, 216 (1980).

8. M. L. Balinski, J. Soc. Industrial and Applied Math., 9, 72 (1961); M. E. Dyer and L. G. Proll, Mathematical Programming, 12, 81 (1977).

9. D. de Fontaine and R. Kikuchi, National Bureau of Standards Publication SP-496, 999 (1977).

TABLE I

Critical temperature for the fcc Ising ferromagnet.

Approximation	$k_B T_c / 12 v_1$
Tetrahedron	0.83544
DT	0.84045
OT	0.83394
DTO	0.82981
High T Expansion	0.81627

TABLE II

Expansion coefficients for specific heat.

	a_n		
n	OT	DTO	Exact.
0	6	6	6
1	48	48	48
2	390	390	390
3	3216	3216	3216
4	26004	26724	26844

Table III

Ground-states for fcc lattices with first and second neighbor pair interaction energies.

ε	Structur-bericht	Symmetry Class	Int. Table	Examples/ designation
$\varepsilon<0$	$L1_0$	s. tetragonal	P4/mmm	CuAu
	$L1_2$	s. cubic	Pm3m	Cu_3Au
$\varepsilon>0.5$	$L1_1$	rhombohedral	$R\bar{3}m$	CuPt
	-	s.c. monoclinic	C2/m	A_2B
$0<\varepsilon<0.5$	-	b.c. tetragonal	$I4_1/amd$	A_2B_2
	-	b.c. orthorhombic	I mmm	Ni_2V, $MoPt_2$
	-	s.c. monoclinic	C2/m	A_2B'
	-	s.c. monoclinic	C2/m	A_2B''
	DO_{22}	b.c. tetragonal	I4/mmm	Ni_3V, $TiAl_3$
$\varepsilon>0$	-	s.c. monoclinic	C2/m	A_5B

Table IV

Ground-states stabilized by many-body interactions in the tetrahedron-octahedron approximation for the fcc lattice.

Designation†	Symmetry Class	Int. Table
AB (a)	s. tetragonal	P4/nmm
AB (b)	s. tetragonal	$P\bar{4}m2$
AB (d)	s. tetragonal	$P4_2/mcc$
AB (e)	s. orthorhombic	Pmmm
AB (f)††	f.c. cubic	Fd3m
AB_2 (c)*	b.c. tetragonal	I4/mmm
A_5B_3 (g)††	b.c. cubic	I432

† See Fig. (1) for two dimensional projections of superstructures.

†† Cubic axis are $2a_o$ <100> with a_o the fcc lattice parameter.

* Tetragonal axis are a = a_o [100], b = a_o [001], c = $2a_o$ [010].

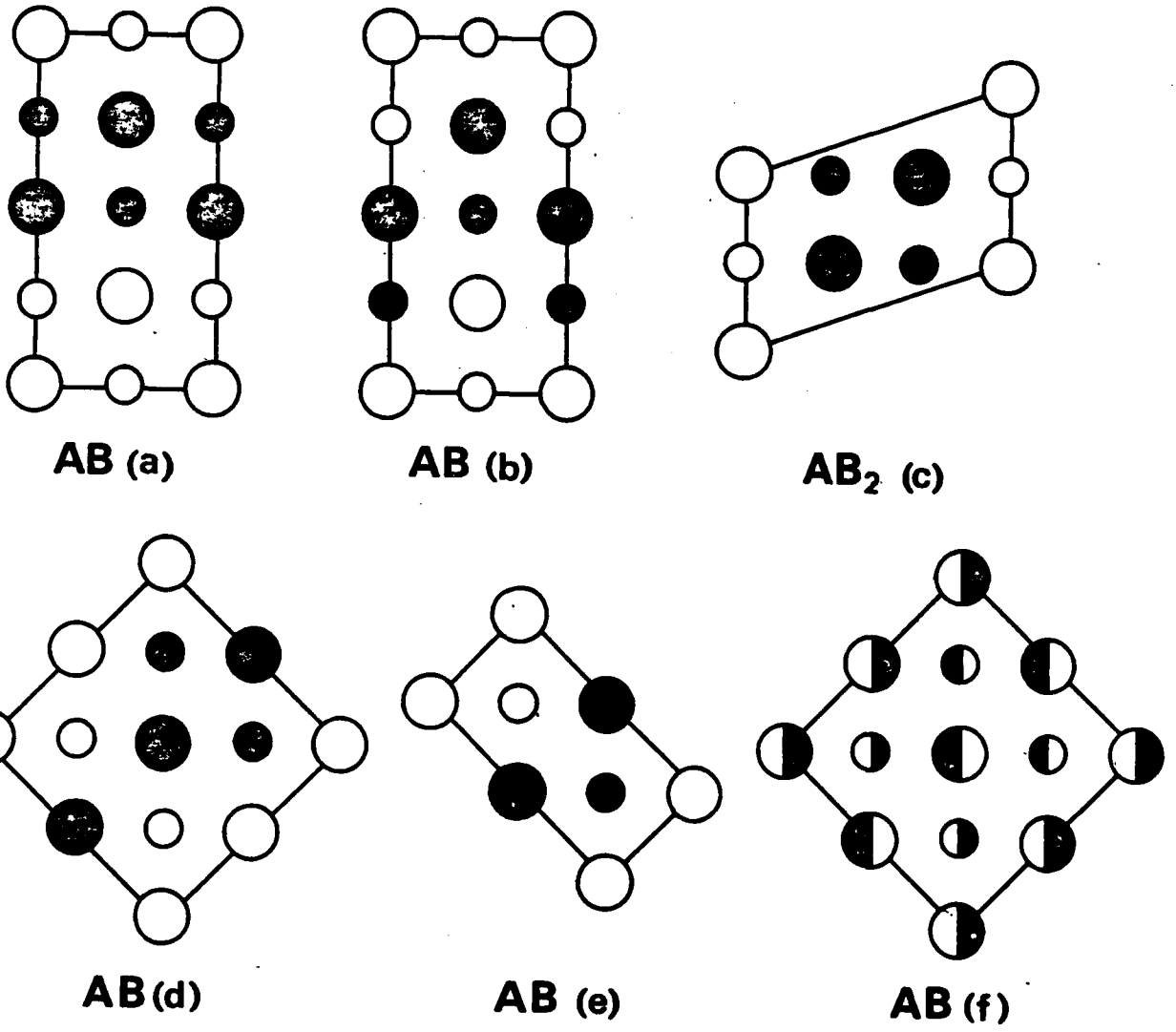

Figure 1

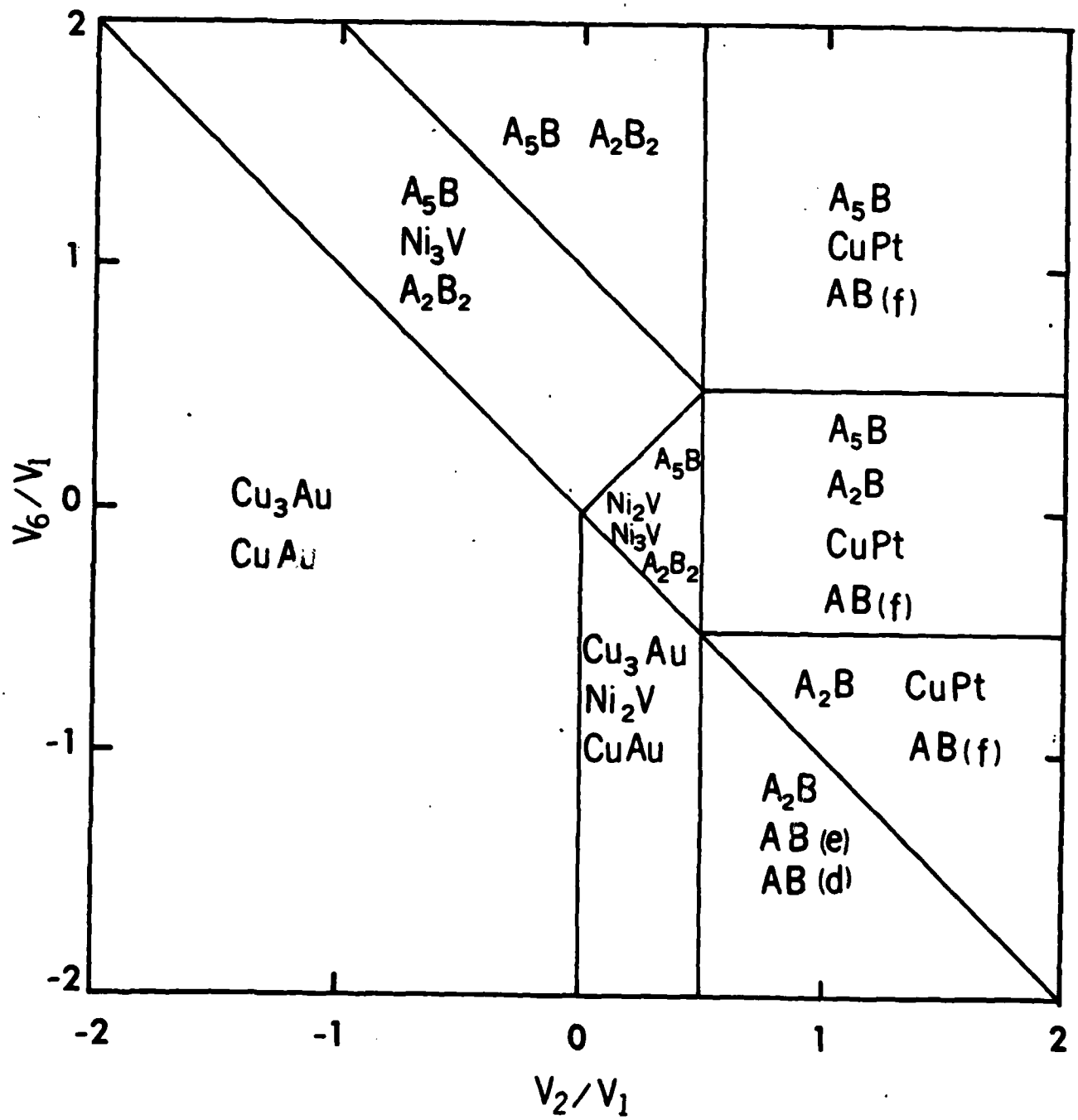
2
1
0
-1
-2
-2
-1
0
1
2
V_6/V_1
V_2/V_1
A_5B A_2B_2
A_5B
Ni_3V
A_2B_2
A_5B
CuPt
AB (f)
A_5B
A_2B
CuPt
AB (f)
A_5B
Ni_2V
Ni_3V
A_2B_2
Cu_3Au
CuAu
Cu_3Au
Ni_2V
CuAu
A_2B CuPt
AB (f)
A_2B
AB (e)
AB (d)

Figure 2

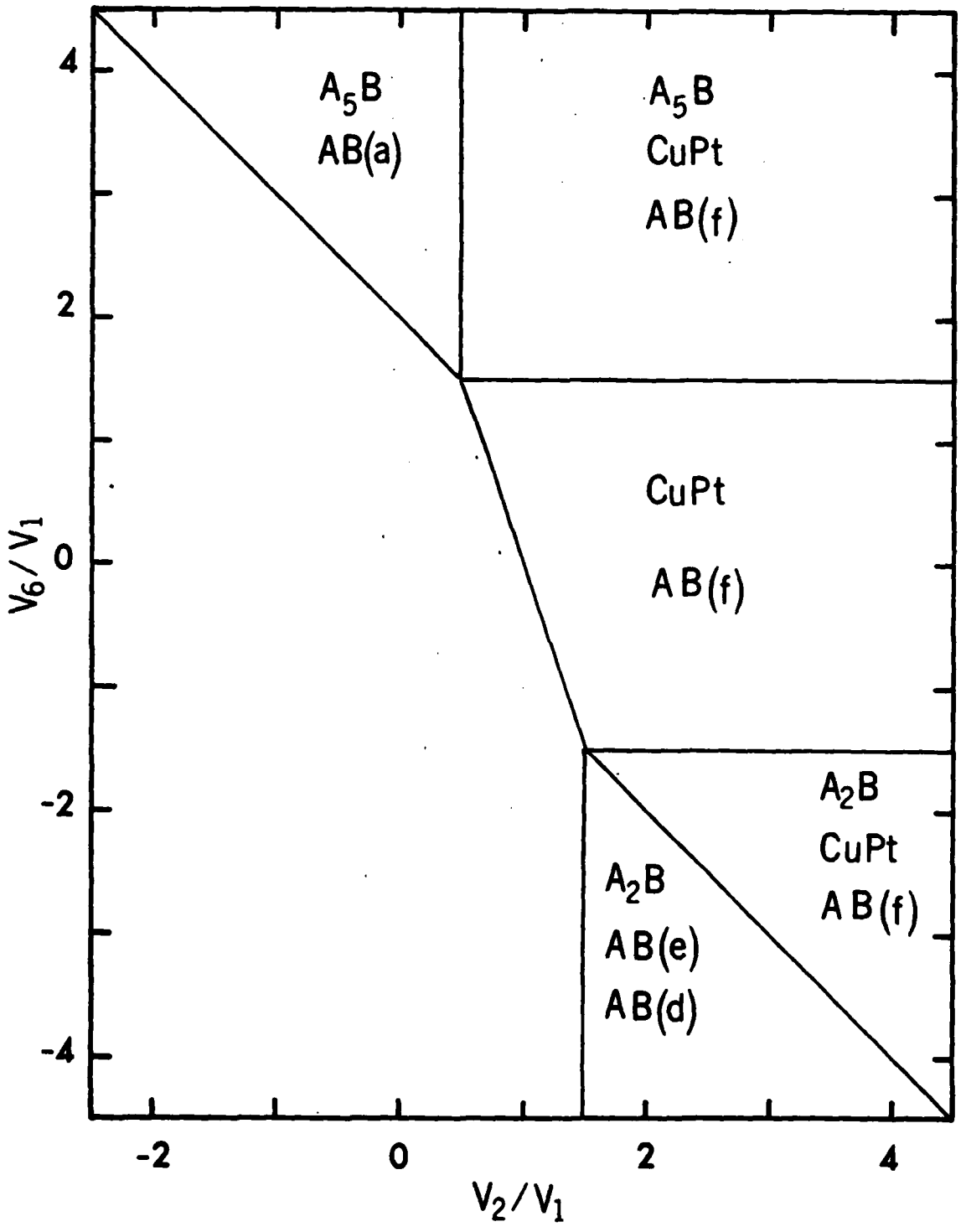
A_5B
AB(a)
A_5B
CuPt
AB(f)
CuPt
AB(f)
A_2B
CuPt
AB(f)
A_2B
AB(e)
AB(d)
4
2
0
-2
-4
V_6/V_1
-2
0
2
4
V_2/V_1

Figure 3

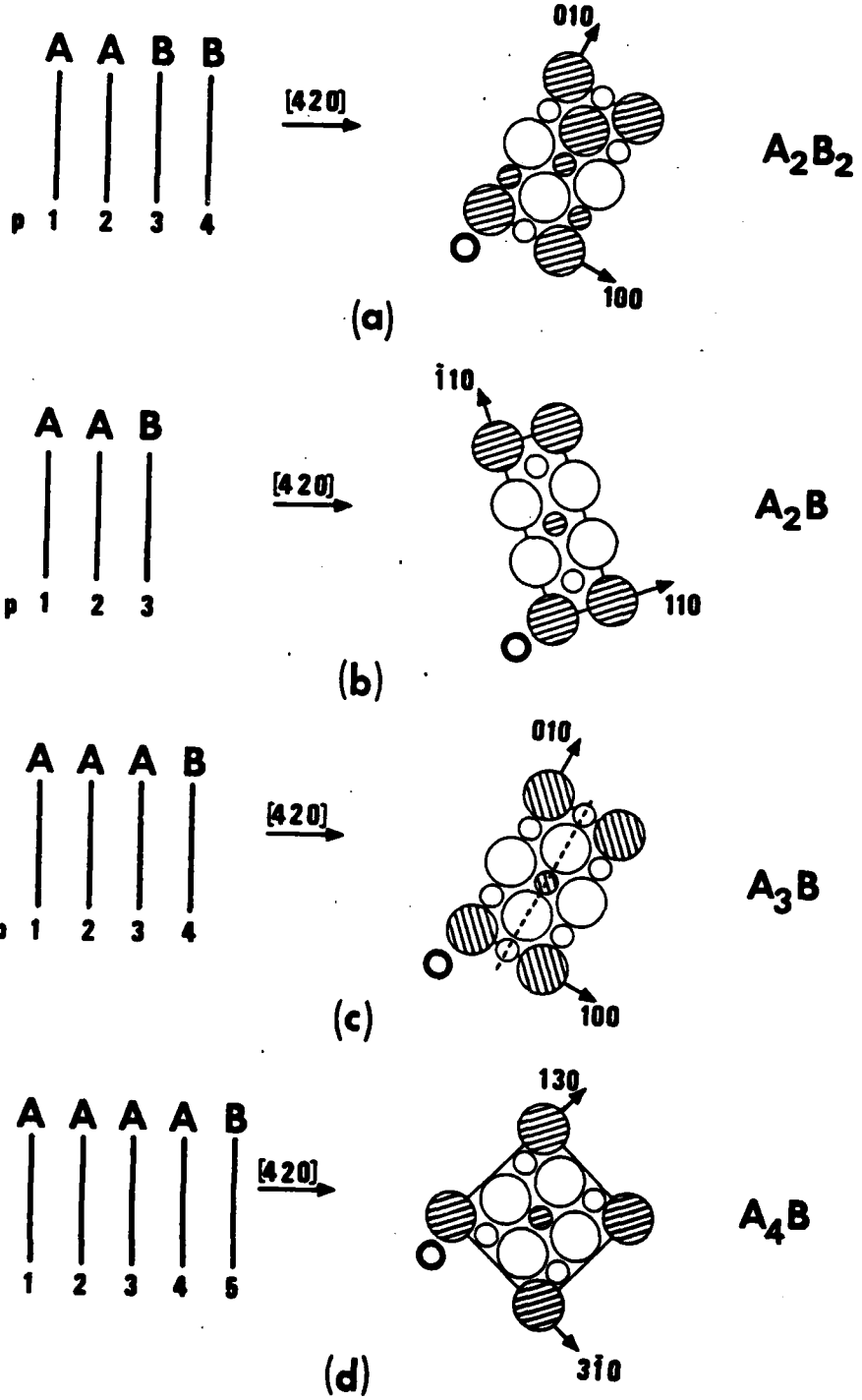
A A B B
p 1 2 3 4
[420]
010
100
O
A_2B_2
(a)
A A B
p 1 2 3
[420]
$\bar{1}10$
110
O
A_2B
(b)
A A A B
p 1 2 3 4
[420]
010
100
O
A_3B
(c)
A A A A B
p 1 2 3 4 5
[420]
130
$3\bar{1}0$
O
A_4B
(d)

Figure 4

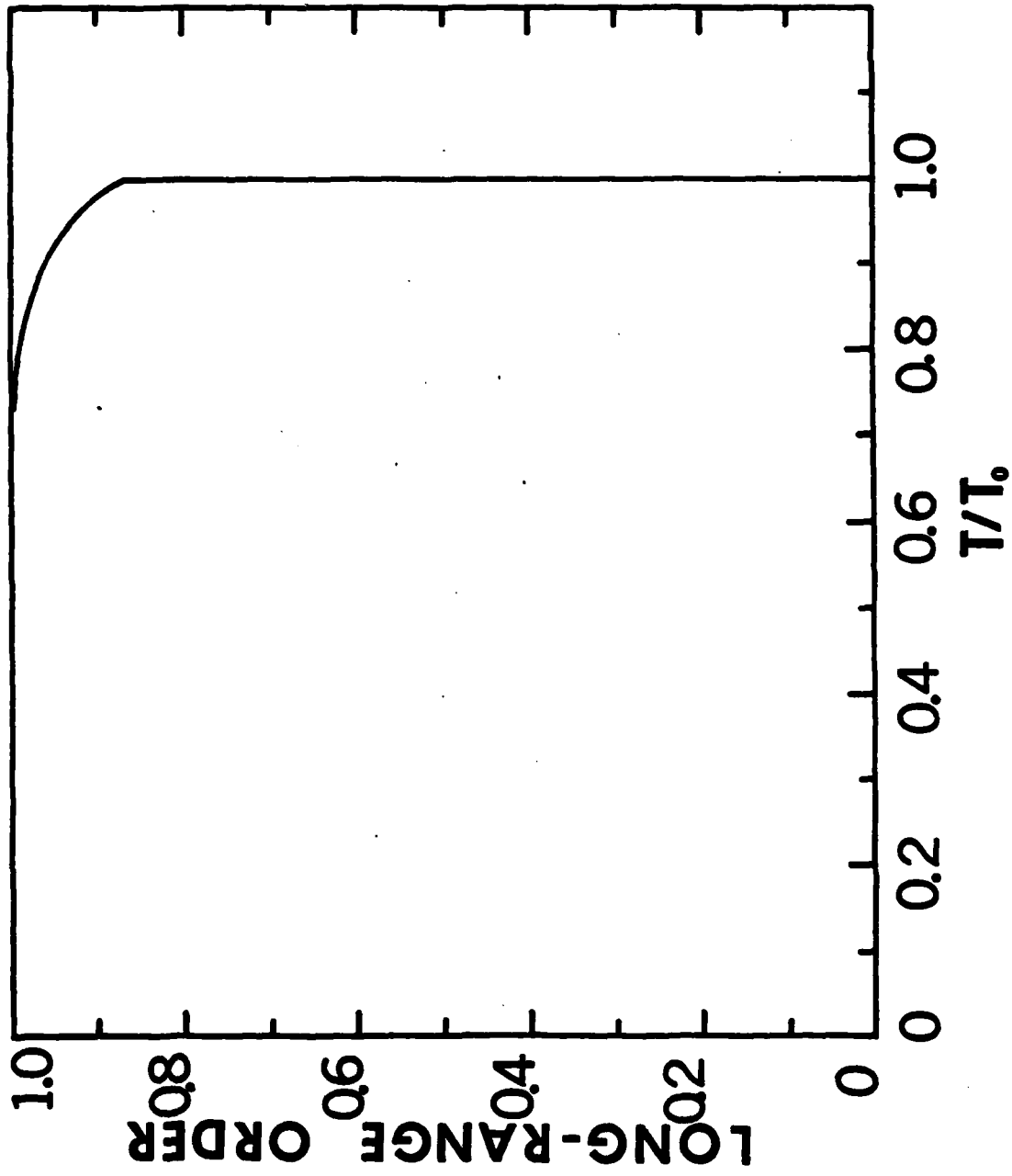

Figure 5

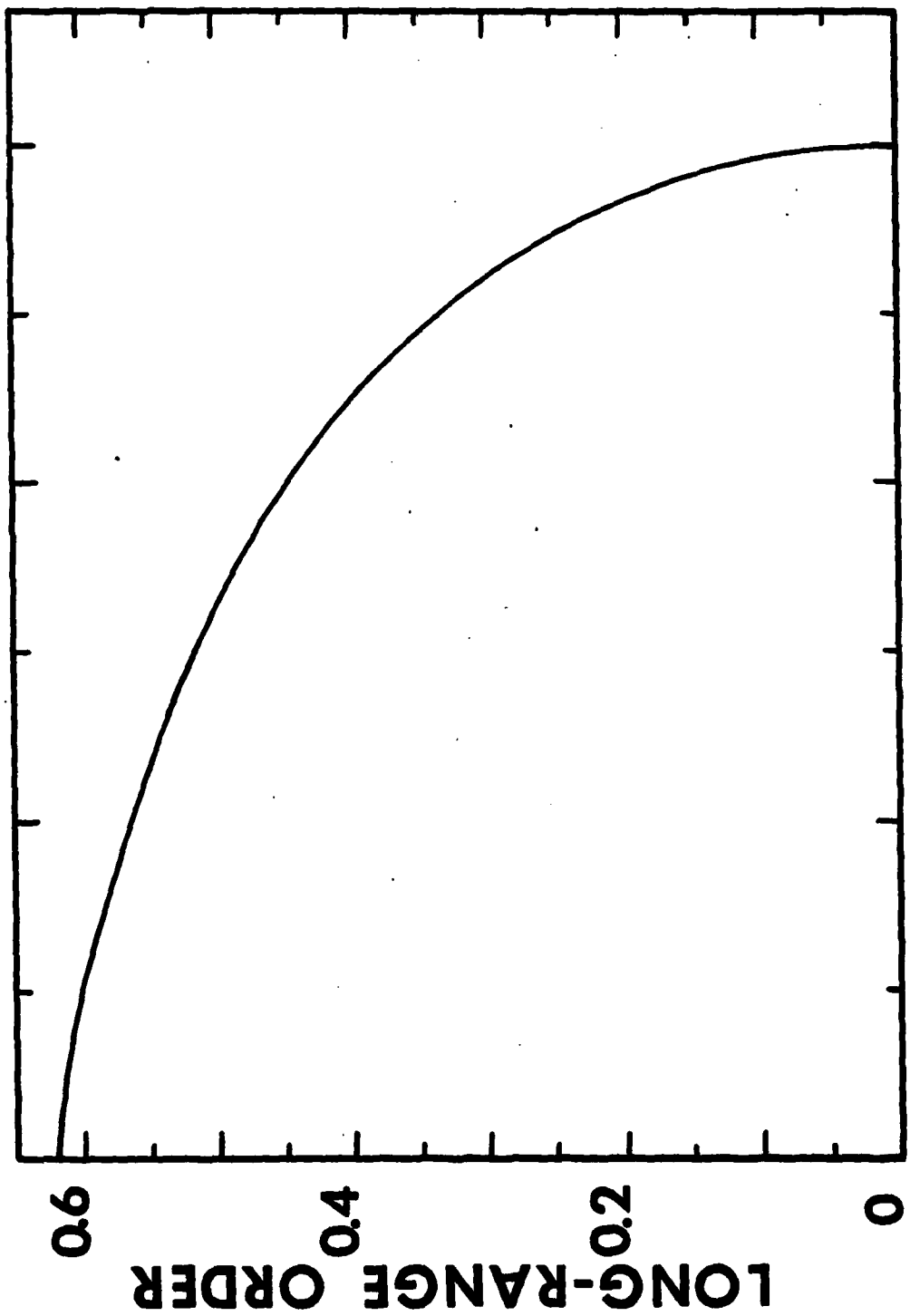

Figure 6

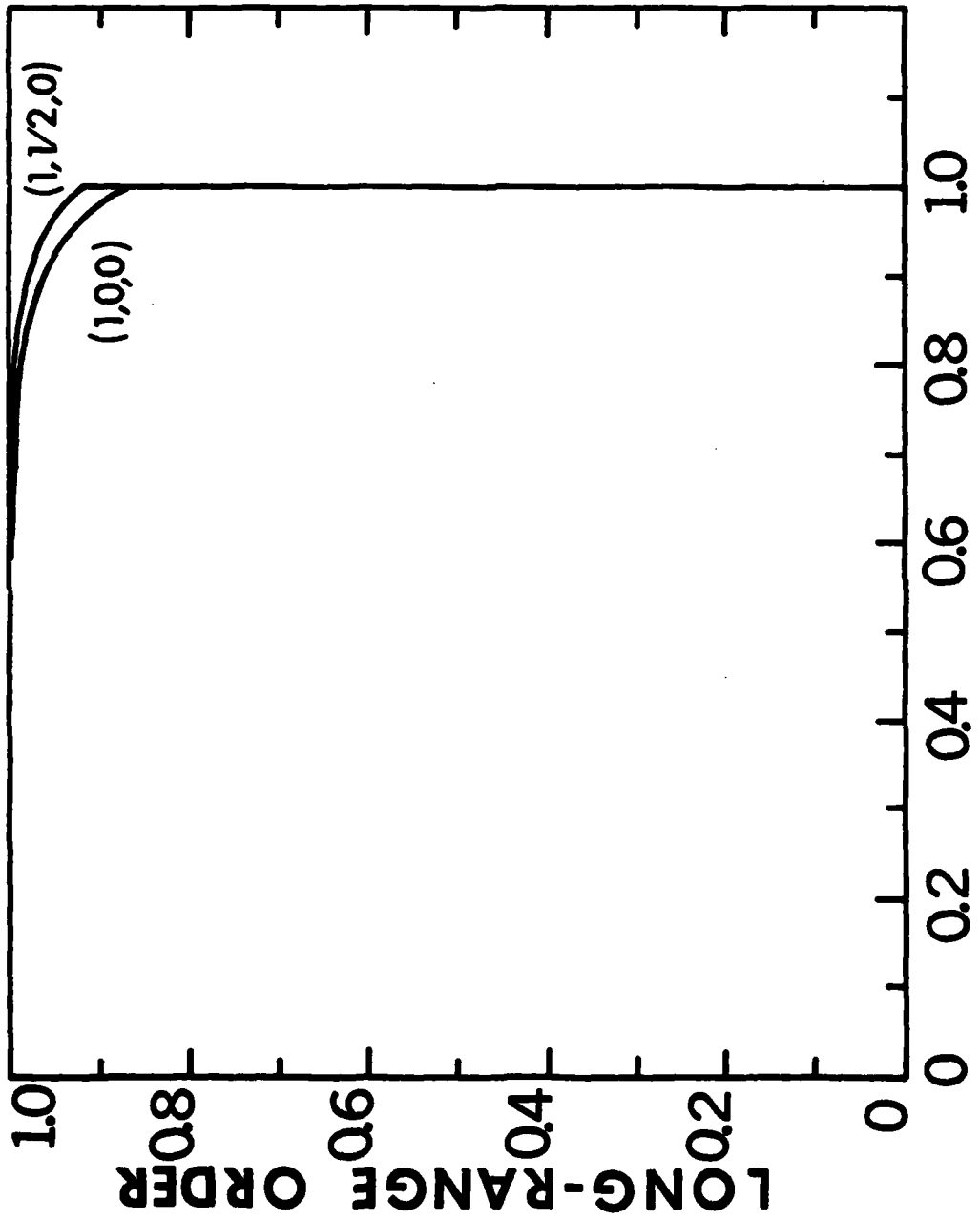

Figure 7

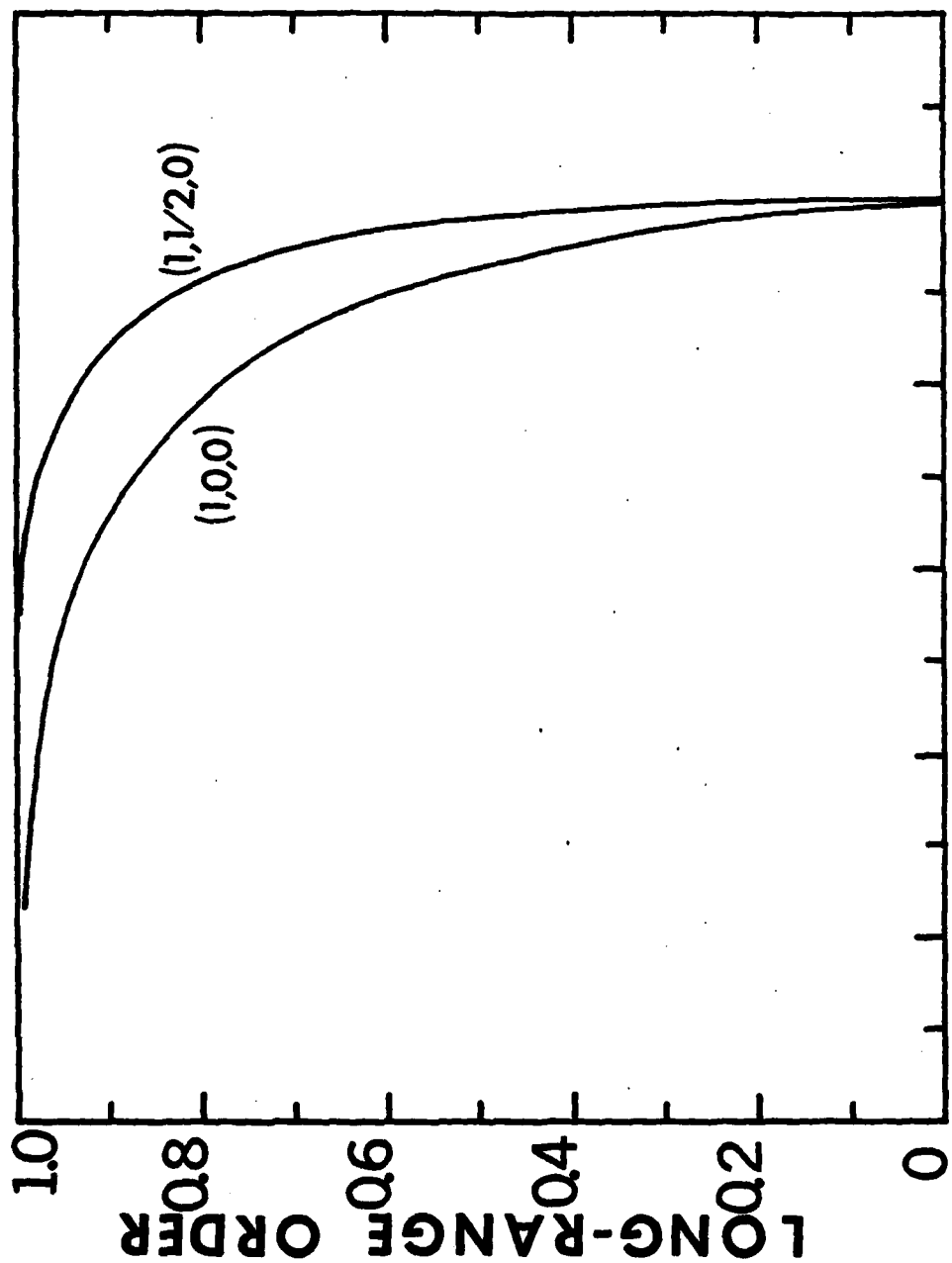

Figure 8

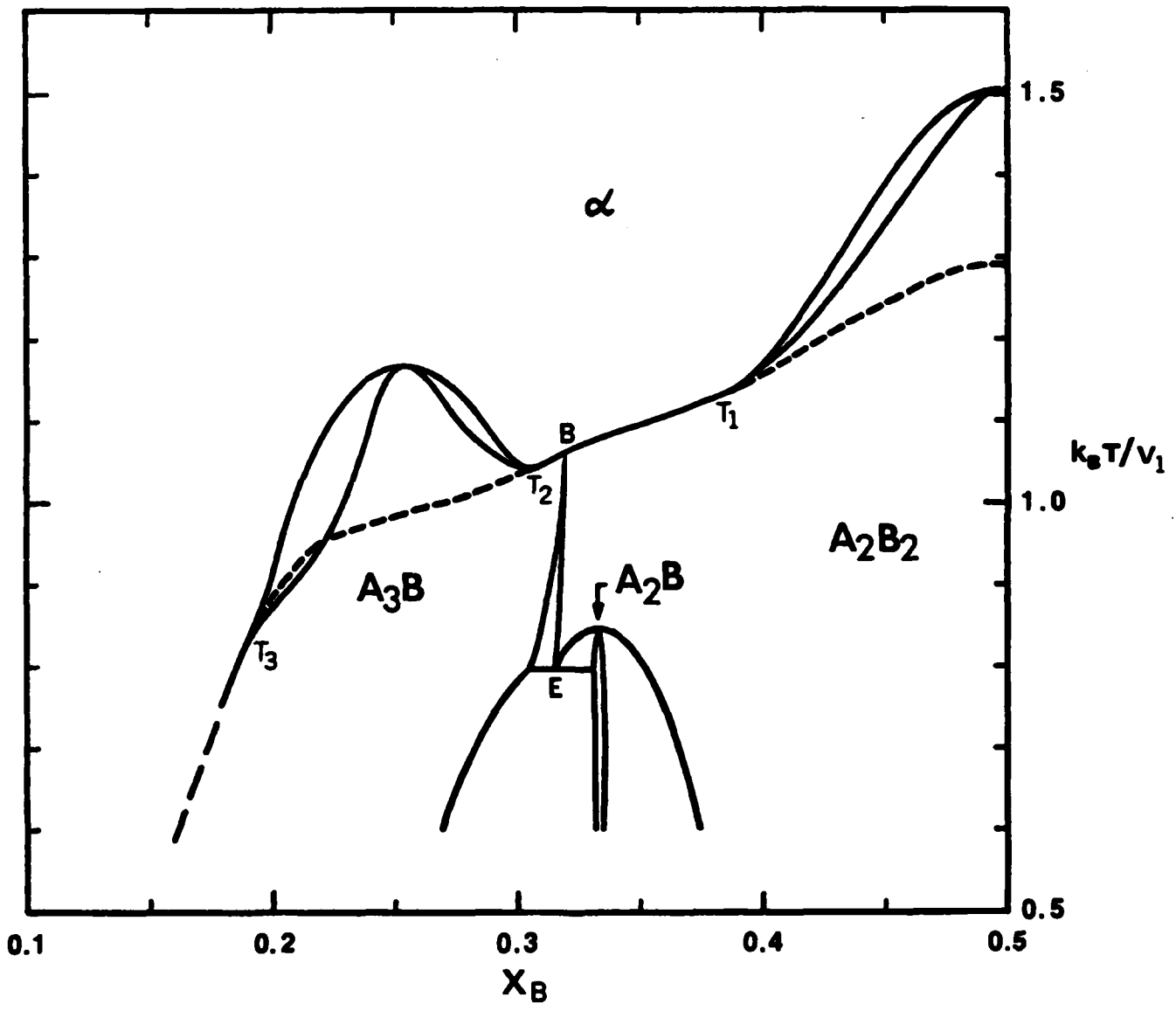

Figure 9

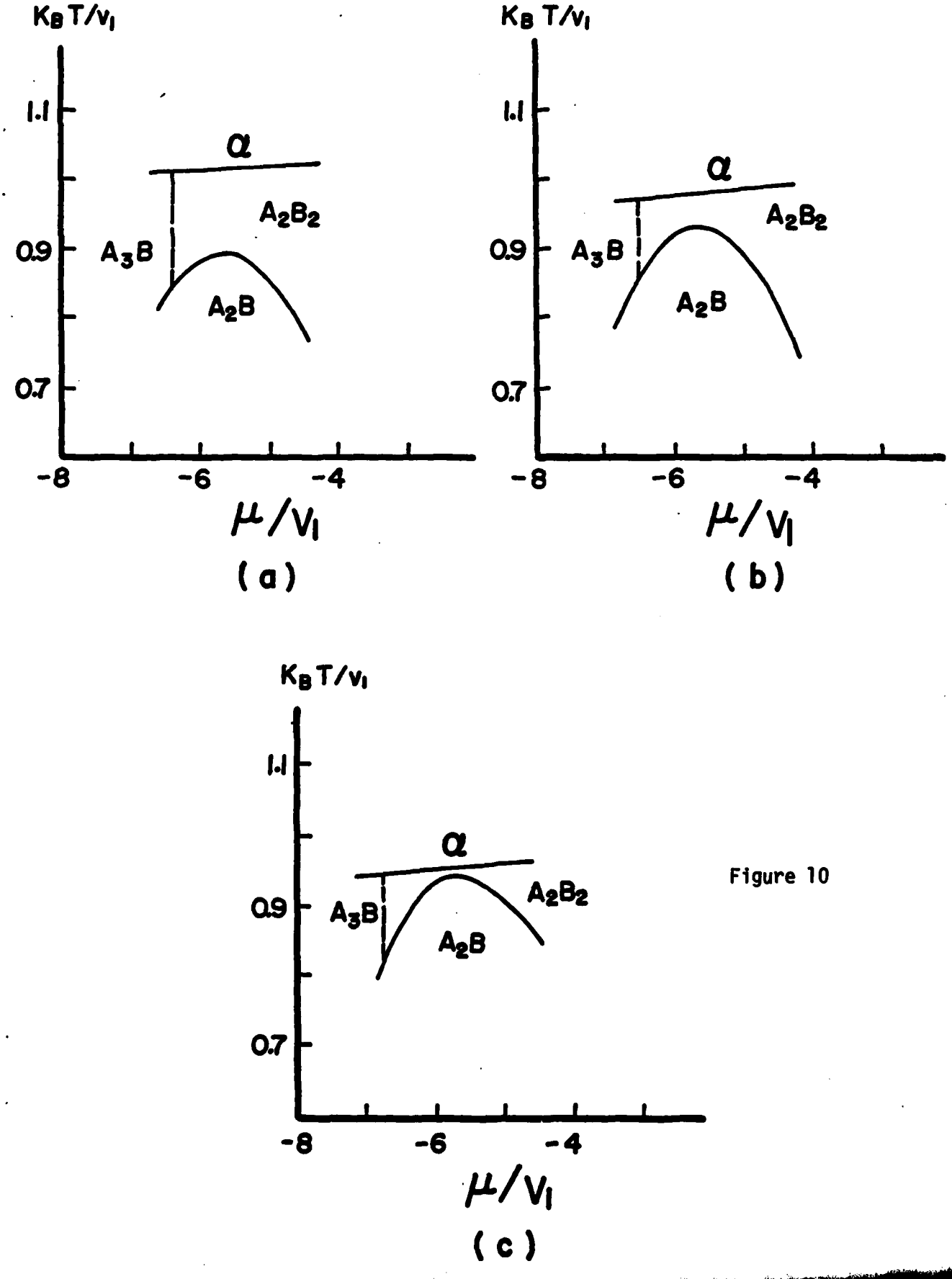
$K_B T/v_l$
1.1
0.9
0.7
α
A_2B_2
A_3B
A_2B
-8
-6
-4
μ/v_l
(a)
$K_B T/v_l$
1.1
0.9
0.7
α
A_2B_2
A_3B
A_2B
-8
-6
-4
μ/v_l
(b)
$K_B T/v_l$
1.1
0.9
0.7
α
A_2B_2
A_3B
A_2B
-8
-6
-4
μ/v_l
(c)

Figure 10

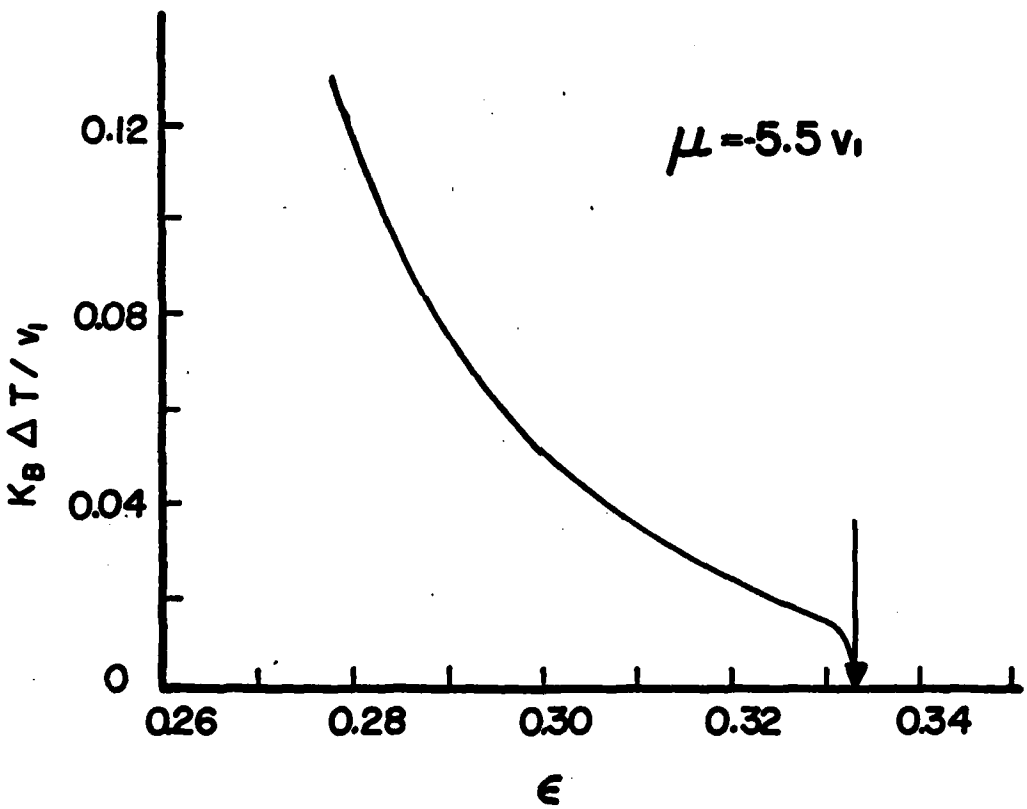

Figure 11

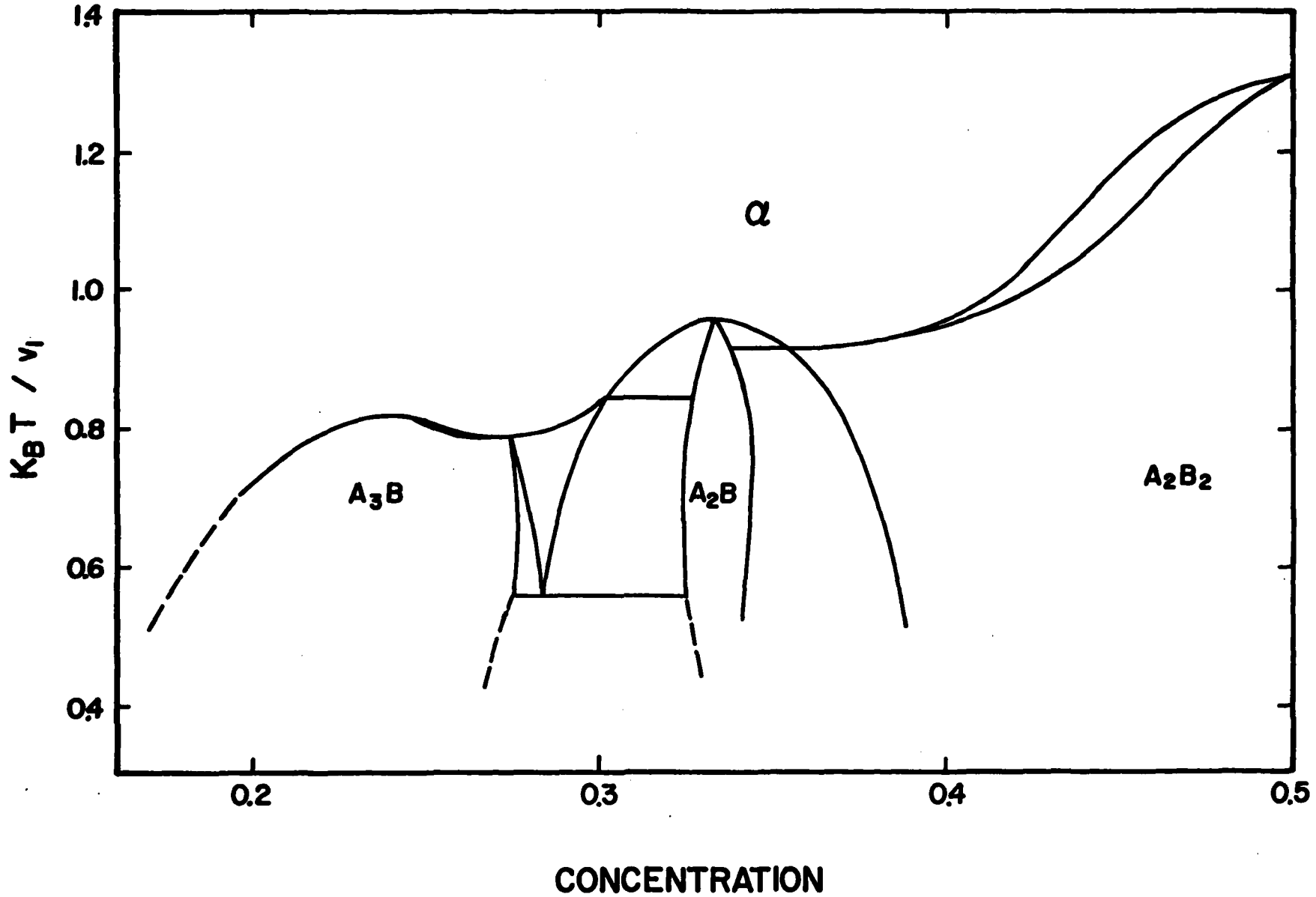

Figure 12

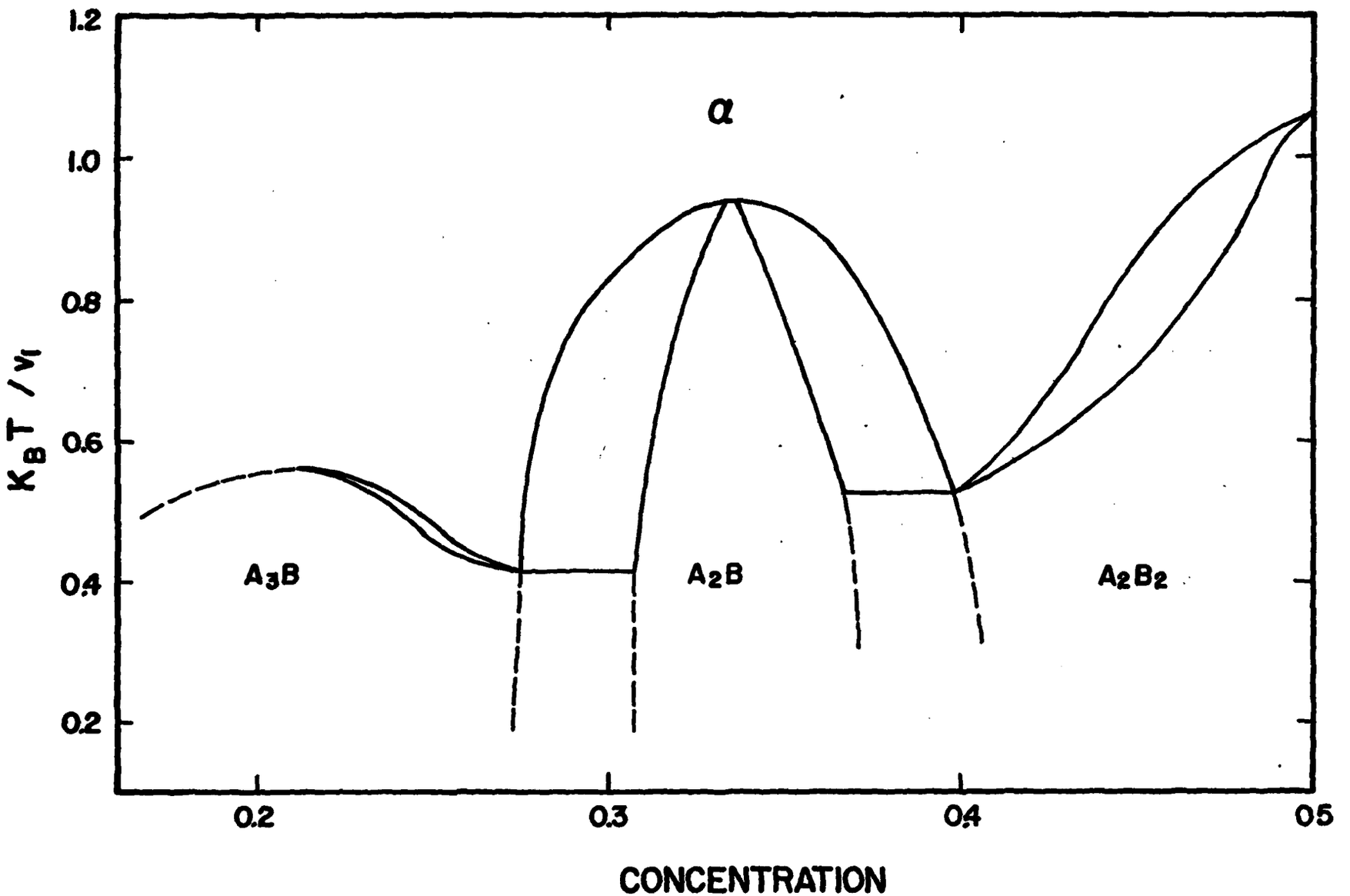

Figure 13

APPENDIX

6. PUBLICATIONS AND PRESENTATIONS

6.1. Publications

Sanchez, J. M. and de Fontaine, D., "The fcc Ising Model in the Cluster Variation Approximation", Phys. Rev. B, 17, 2926 (1978).

Sanchez, J. M. and de Fontaine, D., "Cluster Approach to Order-Disorder Transitions", Modulated Structures - 1979, J. M. Cowley, J. B. Cohen, M. B. Salamon and B. J. Wuensch, eds., AIP Conference Proceedings No. 53, pp. 133-145 (1979).

de Fontaine, D., "Configurational Thermodynamics of Solid Solutions", Solid State Physics, H. Ehrenrich, F. Seitz and D. Turnbull, eds., Vol. 34, Academic Press, New York (1979), pp. 73-272.

de Fontaine, D., "Ordering Instabilities and Pretransitional Effects", Symposium on Pretransitional Phenomena, New Orleans, Feb. 18-22, 1979, to be published in Metallurgical Transactions.

Sanchez, J. M., Kikuchi, R., Yamauchi, H., and de Fontaine, D., "Cluster Approach to Order and Disorder", in Theory of Alloy Phase Formation, L. H. Bennet, ed., 1980.

Sanchez, J. M. and de Fontaine, D., "Ordering in fcc lattices with first- and second-neighbor interactions", Phys. Rev. B, 21, 216 (1980).

Sanchez, J. M. and de Fontaine, D., "Theoretical Prediction of Ordered Superstructures in Metallic Alloys", to appear in Structure and Bonding in Crystals, M. O'Keeffe and A. Navrotsky, eds., Academic Press, New York (1980).

de Fontaine, D., "Spinodal and Equilibrium Reactions", International Symposium on Thermodynamics of Alloys, The Netherlands, June 12-13, 1980, to be published in Physica.

6.2. Oral Presentations

Sanchez, J. M., de Fontaine, D. and Kikuchi, R., "Application of the Cluster Variation Method to Order-Disorder Phase Diagrams", AIME Symposium on Spinodal and Ordering Transformations, Denver, Colorado, February 27, 1978.

de Fontaine, D., "Méthodes récentes de description thermodynamique des phases", Aluminium Pechiney, Voreppe (France), January 18, 1979.

de Fontaine, D., "Ordering Instabilities and Pretransitional Effects", Pretransformation Phenomena, New Orleans, February 19, 1979.

Sanchez, J. M., Kikuchi, R., Yamauchi, H., and de Fontaine, D., "Cluster Approach to Order and Disorder", Symposium on Theory of Alloy Formation, New Orleans, February 19, 1979.

de Fontaine, D., "Structures ordonnées sous l'effet de forces à plusieurs corps", CNRS, Grenoble (France), March 22, 1979.

Sanchez, J. M. and de Fontaine, D., "Cluster Approach to Order-Disorder Transitions", International Conference on Modulated Structures, Kailua-Kona, Hawaii, March 22-25, 1979.

de Fontaine, D., "Détermination de structures ordonnées et diagrammes d'équilibre par le methode des clusters", Dept. of Physics, Univ. of Liège (Belgium), May 7, 1979.

de Fontaine, D., "Détermination de surstructures ordonnées et diagrammes d'équilibre par la méthode des amas", CEN Saclay (France), May 15, 1979.

de Fontaine, D., "La transformation oméga", ONERA, Châtillon (France), May 16, 1979.

de Fontaine, D., "Spinodale d'ordre et phénomènes prémonitoires", CEN Saclay (France), May 17, 1979.

de Fontaine, D., "Interactions elastiques dans les solides", CEN Saclay (France), May 18, 1979.

de Fontaine, D., "Etudes des transformations ordre-désordre par la méthode des amas", Ecole Polytechnique Fédérale, Lausanne (Switzerland), June 25, 1979.

de Fontaine, D., "Thermodynamique des amas et phases ordonnées", Dept. of Physics, Univ. of Strasbourg (France), June 29, 1979.

de Fontaine, D., "Diagrammes d'équilibre et métastabilité", Univ. of Poitiers, Dept. of Metallurgy (France), July 3, 1979.

Sanchez, J. M., "Teoria de Ordem-Desordem en Solidos", Annual Meeting Sociedade Brasileira de Cristalografia, Recife, Brazil, July 18-21, 1979.

Sanchez, J. M., "The Cluster Variation Method", Centro Brasileiro de Pesquisas Fisicas, Rio de Janeiro, Brazil, August 10, 1979.

Sanchez, J. M., "Classical Approach to Order-Disorder", Instituto de Fisica, Universidade de São Paulo, Brazil, October 29, 1979.

de Fontaine, D., "Prediction of Coherent Phase Equilibria in Alloys", School of Eng. Appl. Sc., UCLA, December 7, 1979.

de Fontaine, D., "Prediction of Ordered Superstructures in Metallic Alloys", Conf. on Crystal Chemistry of Complex Solids, Univ. of Arizona, January 25, 1980.